

## ***In-situ* Monitoring of Anodic Oxidation of p-type Si(100) by Electrochemical Impedance Techniques in Nonaqueous and Aqueous Solutions**

Min-Soo Kim, Kyung-Ku Kim, Sang Youl Kim,<sup>†</sup> Youngtae Kim,<sup>†</sup> Young Hee Won,<sup>†</sup>  
Yeorn-Ik Choi,<sup>‡</sup> and Sun-il Mho\*

Department of Chemistry, <sup>†</sup>Department of Physics, <sup>‡</sup>Department of Electrical Engineering,  
Ajou University, Suwon 442-749, Korea

Received June 22, 1998

Electrochemical oxidation of silicon (p-type Si(100)) at room temperature in ethylene glycol and in aqueous solutions has been performed by applying constant low current densities for the preparation of thin SiO<sub>2</sub> layers. *In-situ* ac impedance spectroscopic methods have been employed to characterize the interfaces of electrolyte/oxide/semiconductor and to estimate the thickness of the oxide layer. The thicknesses of SiO<sub>2</sub> layers calculated from the capacitive impedance were in the range of 25-100 Å depending on the experimental conditions. The anodic polarization resistance parallel with the oxide layer capacitance increased continuously to a very large value in ethylene glycol solution. However, it decreased above 4 V in aqueous solutions, where oxygen evolved through the oxidation of water. Interstitially dissolved oxygen molecules in SiO<sub>2</sub> layer at above the oxygen evolution potential were expected to facilitate the formation of SiO<sub>2</sub> at the interfaces. Thin SiO<sub>2</sub> films grew efficiently at a controlled rate during the application of low anodization currents in aqueous solutions.

### **Introduction**

The growth of ultrathin gate oxide SiO<sub>2</sub> films of good electrical properties is a key concern for silicon-based semiconductor industries.<sup>1,2</sup> To form ultrathin oxide layers, low temperature processing is required to restrict dopant impurity diffusion, although high temperature thermal oxidation of Si surfaces has been used for many years to produce silicon oxides.<sup>3,4</sup> A different course for the thermal growth of SiO<sub>2</sub> at high temperatures is the electrochemical oxidation of silicon at room temperature.<sup>5-12</sup> A potential advantage of the electrochemical methods over the thermal process includes the precise control over the deposition rate at relatively low temperatures. Also, electrochemical techniques for fabricating and modifying semiconductors have recently begun to show promise as practical substitutes for high vacuum techniques, which have been the source of information on the growth and surface morphologies of semiconductors.<sup>13,14</sup> The properties of the Si/SiO<sub>2</sub> interfaces help determine the performances of semiconductor devices and are sensitive to the methods used for preparation. The electrochemical oxidation technique may offer a variety of possibilities to control the interface properties. Most of the previous work on the growth of the anodic oxides have been processed with relatively high current densities and the oxides electrical properties have been investigated extensively by various *ex-situ* techniques.<sup>1,4,8-11,16</sup> Bardwell *et al.* used the electrochemical method to prepare thin SiO<sub>2</sub> layer on Si at room temperature in aqueous NH<sub>4</sub>OH solution,<sup>11,13,17</sup> characterizing electrochemically grown SiO<sub>2</sub> films and comparing them with thermally grown SiO<sub>2</sub> films, using ac impedance and x-

ray photoelectron spectroscopy<sup>13</sup>. They applied a constant anodic potential in the 1 V to 9 V range for a fixed period of time. They used the capacitive value obtained from the impedance data to obtain the thickness of the SiO<sub>2</sub> layer on Si. In the present work, electrochemical oxidation of silicon (p-type Si(100)) at room temperature both in ethylene glycol and in aqueous solution has been conducted with low current densities to prepare SiO<sub>2</sub> layers. Low current densities are preferred to grow an ultrathin oxide layer ( $\leq 100$  Å) with high current efficiencies. Also, by applying constant current densities, constant controlled rates of electrochemical reaction could be forced at the electrode interfaces. Hence, the thickness of the dielectric layer would be controlled by the anodization time, which is monitored by *in-situ* electrochemical impedance techniques as a function of anodization time. It is the aim of this work to employ *in-situ* ac impedance methods to characterize electrolyte/oxide/semiconductor (EOS) interfaces and to investigate the growth mechanism of the anodic oxides. Space charge capacitance of the accumulation layer in the Si electrode is also included in the equivalent circuit to estimate the thickness of the thin dielectric SiO<sub>2</sub> layer both in aqueous and nonaqueous solutions.

### **Experimental Section**

Anodic oxides on p-type Si((100), 10 Ωcm) wafer were grown by electrochemical oxidation in aqueous solutions of ammonium hydroxide (1.35 M) and in nonaqueous (ethylene glycol) solution containing 0.04 M KNO<sub>3</sub>. A conventional three electrode configuration was used: a 1×1 cm silicon wafer as a working electrode, a platinum gauze counter electrode and a Ag/AgCl (KCl saturated) reference electrode. Silicon electrode surfaces were cleaned, etched,

\*Corresponding author: e-mail: mho@madang.ajou.ac.kr Tel: +82-331-219-2599 Fax: +82-331-219-1615.

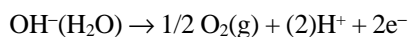
and rinsed, sequentially, in a (5 : 1 : 1 H<sub>2</sub>O : NH<sub>4</sub>OH : H<sub>2</sub>O<sub>2</sub>) cleaning solution, a (1 : 50 HF : H<sub>2</sub>O) etching solution, and a (6 : 1 : 1 H<sub>2</sub>O : HCl : H<sub>2</sub>O<sub>2</sub>) cleaning solution, and rinsed thoroughly with distilled deionized water in between and after each process. Electrical contact was made first by smearing InGa eutectic paste onto the back side of the wafer and second by using silver paste to connect to wires. The edges and back of the wafer were sealed with a silicon sealant after the electrical contact. Electrode potentials reported here refer to the reference electrode. Anodic oxidation of the Si wafer was processed by applying low current densities of 10  $\mu\text{A}/\text{cm}^2$  and 30  $\mu\text{A}/\text{cm}^2$  (galvanostatically). The corresponding potential at the Si electrode was measured by using a potentiostat/galvanostat (EG&G Model 173 interfaced to a computer with a Model 276A Interface). *In-situ* ac impedance technique using a Zahner (Model IM6) setup has been employed to evaluate the interface characteristics of electrolyte/oxide/semiconductor (EOS) structures. Impedance was measured every 5 minutes during anodization. Impedance measurements were carried out in the same electrolyte solutions by applying 10 mV<sub>p-p</sub> ac signal in the 0.1 Hz-100 kHz frequency range on the top of a dc voltage (+0.8 V in aqueous solutions or +1.2 V in nonaqueous solutions). Further oxidation of Si surfaces during the impedance measurement period was prevented by holding a much less anodic potential (0.8 V or 1.2 V) compared with the potential of oxide formation. The measured impedance data were numerically fit to appropriate equivalent electrical circuits using the complex nonlinear least squares fit procedure provided by Zahner Inc. The thickness of the anodic oxide formed galvanostatically at certain anodic current densities for various anodization times was calculated from the capacitive value in the equivalent circuit constructed for the impedance data measured. To make a comparison of the obtained values for the SiO<sub>2</sub> thickness by the ac impedance technique with spectroscopic methods, ellipsometric measurements were employed using a spectroscopic ellipsometer Jobin-Yvon UVISEL.

## Results and Discussion

The overall equation for the anodic oxidation of silicon with water, which is the main source of oxygen, may be written as



Croset *et al.* observed that most of oxygen for the oxide comes from water even in ethylene glycol solutions.<sup>12</sup> The organic molecules do not act as a direct source of oxygen in anodic oxidation of silicon. Also, the current efficiency of the anodic oxidation of silicon is known to be very low at high current densities, since most of the current is used up in evolving oxygen by decomposing the water.



The consecutive steps of the oxidation of silicon in alkaline solution can be envisaged by the initial formation of hydroxide from water:<sup>1</sup>

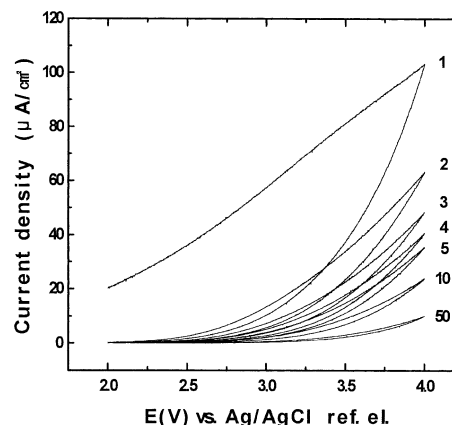
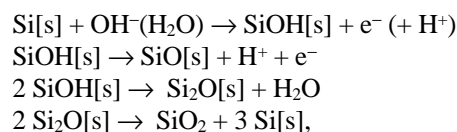


**Figure 1.** The first through fifth, tenth and fiftieth cyclic voltammograms (CVs) of Si electrode in aqueous solution of ammonium hydroxide (1.35 M) among consecutive 50 cycles are overlaid. The scan rate is 50 mV/s.



where, [s] represents the surface site. The consecutive cyclic voltammograms (CVs) of the Si electrode in 1.35 M NH<sub>4</sub>OH solution in the voltage range of silicon oxidation and oxygen

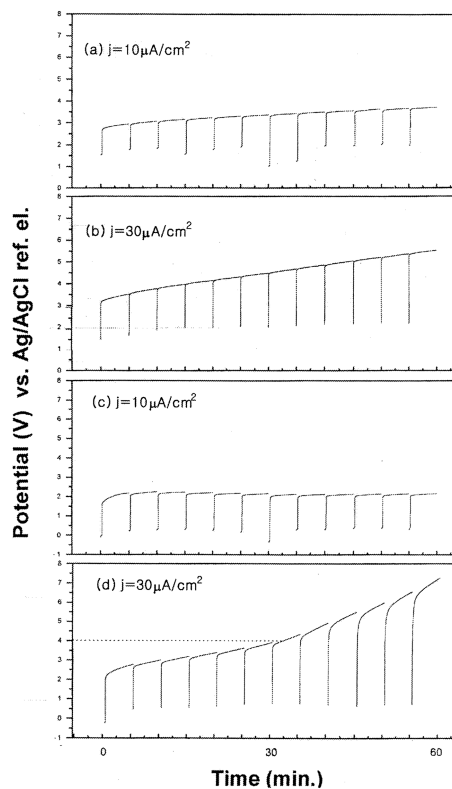


**Figure 2.** Measured potentials as a function of anodization time with applying constant anodic currents of (a) 10  $\mu\text{A}/\text{cm}^2$  and (b) 30  $\mu\text{A}/\text{cm}^2$  in ethylene glycol solution containing 0.04 M KNO<sub>3</sub>, and of (c) 10  $\mu\text{A}/\text{cm}^2$  and (d) 30  $\mu\text{A}/\text{cm}^2$  in aqueous solution of ammonium hydroxide (1.35 M).

evolution are shown in Figure 1. The anodic current increases as the voltage scans toward the anodic direction, where the oxygen evolves and the Si electrode is oxidized. Since there is no specific anodic peaks in CVs of the Si electrode in aqueous and nonaqueous solutions, it is difficult to study mechanism or processes of the oxidation of silicon separately from the whole anodic processes occurring at the electrode interfaces. As the number of cycles of CVs increases, the oxidation current decreases gradually. Both Si surface oxidation and oxygen evolution rates decrease as the oxide layer is formed. High resistance of the oxide layer formed at the electrode surface results in the small slopes in CVs.

Anodic oxidation of Si surfaces is processed galvanostatically. During the anodizing process of Si surfaces galvano-

statically in ethylene glycol containing 0.04 N  $\text{KNO}_3$  and in aqueous  $\text{NH}_4\text{OH}$  solutions, the potentials are monitored as a function of anodization time (chronopotentiometry) as shown in Figure 2. Continuous measurements of potentials are interrupted every 5 minutes to measure the impedance to monitor the interface characteristics. The potential depends upon the applied current, the electrolyte solution, and the anodization time. With an anodic current of  $10 \mu\text{A}/\text{cm}^2$  in ethylene glycol and in aqueous solutions (Figures 2a and 2c), the potential increases during the first 5 minutes of oxidation and then it remains almost constant or increases slightly as the anodization time increases. Silicon oxide seems to form on the Si surfaces during the first 5 minutes of the oxidation period and the oxide film does not grow further at this low current densities. This low current may cor-

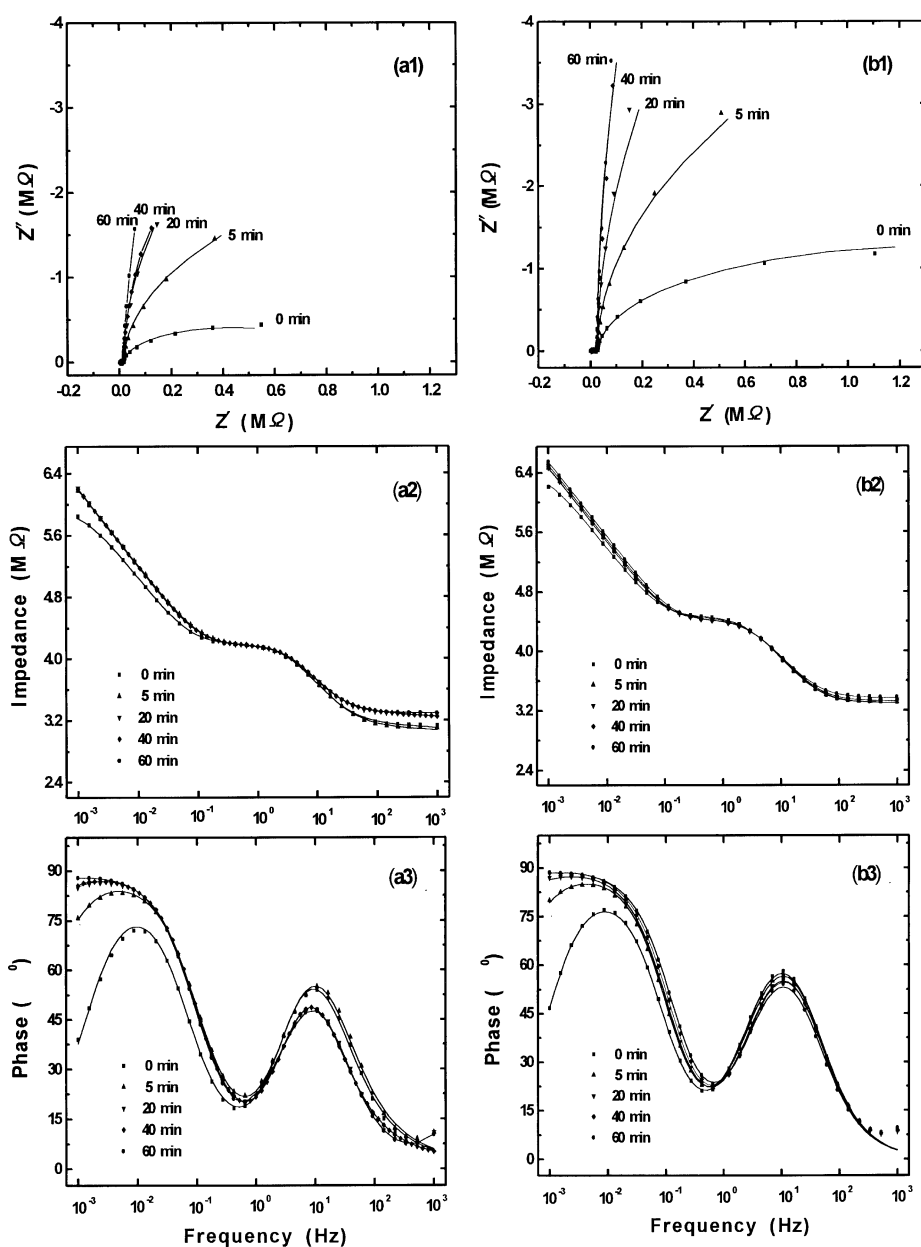


**Figure 3.** Nyquist(1) and Bode (2, 3) plots of the impedance data points and fitted lines obtained during the anodization processes in ethylene glycol solution containing 0.04 M  $\text{KNO}_3$  with applying anodizing currents of (a)  $10 \mu\text{A}/\text{cm}^2$  and (b)  $30 \mu\text{A}/\text{cm}^2$ .

respond to the Fowler-Nordheim tunneling current through a very thin dielectric SiO<sub>2</sub> layer between Si and the electrolyte.<sup>14</sup> The monitored potential increases as the anodization proceeds at the anodic current of 30  $\mu\text{A}/\text{cm}^2$  (Figures 2b and 2d). The oxide layer is expected to grow steadily at this current density.

The growth of oxides on Si in nonaqueous and aqueous solution has been monitored by ac impedance techniques every 5 minutes during anodization. Electrochemical impedance spectra displayed both in Nyquist and Bode plots are shown in Figure 3 for ethylene glycol and Figure 4 for aqueous solutions. As the anodization proceeds, the impedance at the low frequency region changes, which is clearly shown in Nyquist plots (Figures 3a1, 3b1, 4a1, and 4b1). Even when

applying the low anodic current of 10  $\mu\text{A}/\text{cm}^2$ , the impedance at the low frequency region increases (Figure 3a2 and 4a2). The imaginary part of the impedance ( $Z''$ ) at the low frequency region increases with the increasing arc of the hemicircular shape as a result of the increasing real part resistance ( $Z'$ ) parallel to the capacitive component. The resistance corresponds to the sum of the oxide (SiO<sub>2</sub>) resistance and the anodic polarization resistance,  $R_{\text{ox+p}}$ . In ethylene glycol solution, the impedance at low frequencies approaches that of a capacitor, which implies that the sum of the oxide resistance and the polarization resistance ( $R_{\text{ox+p}}$ ) that are parallel with the capacitor approaches a very large value for long periods of anodization, resulting in an open circuit parallel with the capacitor (Figure 3a and 3b). The

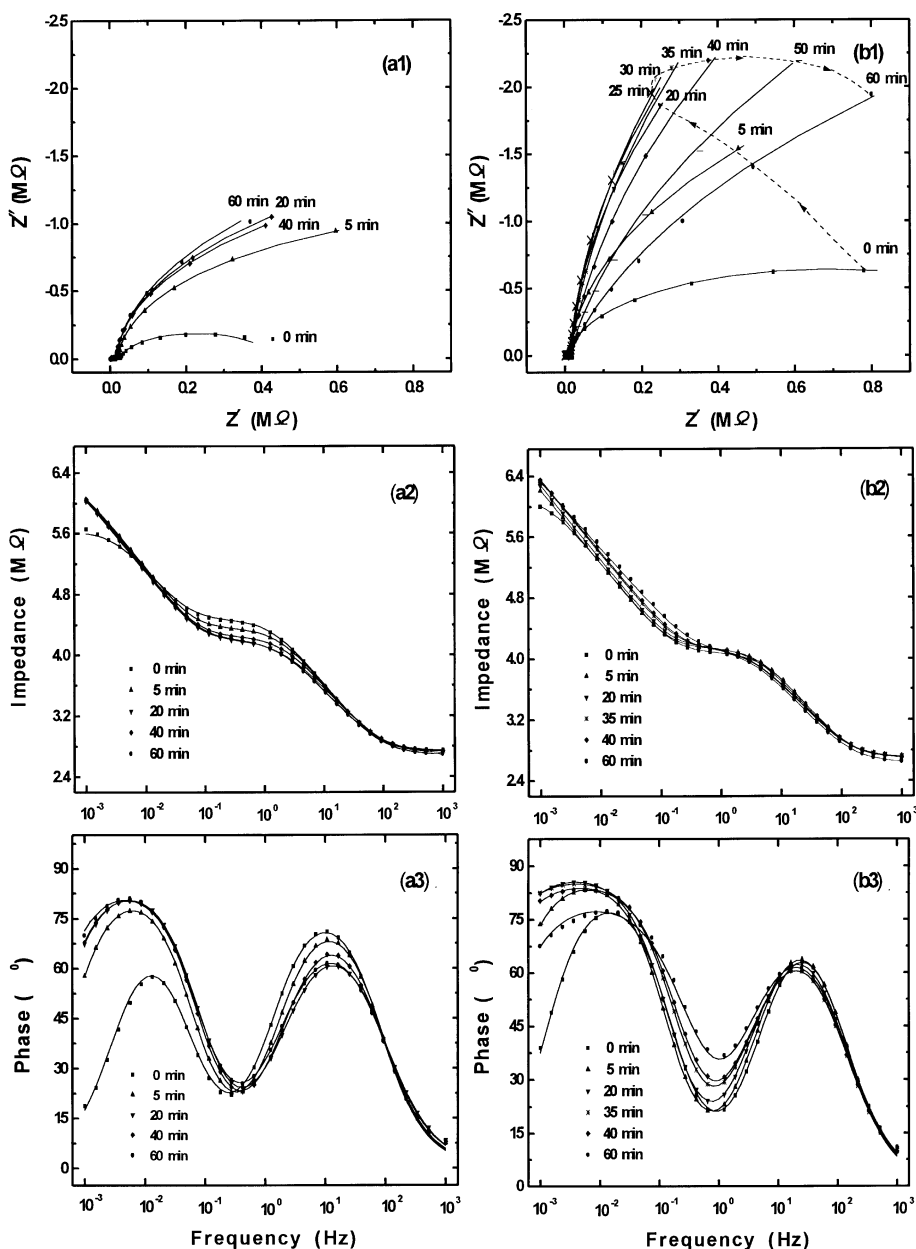


**Figure 4.** Nyquist (1) and Bode (2, 3) plots of the impedance data points and fitted lines obtained during the anodization processes in aqueous ammonium (1.35 M) solution with applying anodizing currents of (a) 10  $\mu\text{A}/\text{cm}^2$  and (b) 30  $\mu\text{A}/\text{cm}^2$ .

oxide layer forms during the first 5 minutes of the anodization period and there is virtually no net increase in film thickness by further anodization in both aqueous and nonaqueous solutions at this low current density, as discussed above with the chronopotentiometric results. Hence, the oxide resistances ( $R_{ox}$ ) increase during the first 5 minutes of the anodization period and are not expected to change with further anodization. The anodic polarization resistance ( $R_p$ ) for the oxidation of silicon and oxygen evolution from water contained in the nonaqueous solution increases to very large values (Figure 3a). The anodic polarization of water at the interfaces is expected to increase substantially because of the finite content of water in the solution. On the other hand, the change in impedance in aqueous solutions as the anodization proceeds at this low current density ( $10 \mu\text{A}/\text{cm}^2$ ) is comparatively small (Figure 4a).

With the current densities of  $30 \mu\text{A}/\text{cm}^2$ , the monitored potential increases continuously up to 10 V, which is the limiting potential of the potentiostat. The impedance at low frequencies increases continuously as the anodization time increases in ethylene glycol solution, as shown in Figure 3b. In the ethylene glycol solution, not only does the oxide film grow but the anodic polarization resistance increases continuously because of the finite water content in the solution. In aqueous solutions, the impedance at the low frequency region increases (Figure 4b2). Interestingly, the phase angle of the impedance at low frequencies increases at the beginning of anodization processes and decreases with further anodization (Figure 4b3). The trend of change in impedance spectra in aqueous solution shows an obvious deflection in Nyquist plots as the anodization time increases at the applied current densities of  $30 \mu\text{A}/\text{cm}^2$  (Figure 4b1). In Figure 4b1, at up to 30 minutes of anodization, where the monitored potentials are below 4 V, the imaginary part of the impedance ( $Z''$ ) increases with the increase of the arc of the hemicircular shape resulting from the increasing real part value ( $Z'$ ) parallel to the capacitive part of the impedance. However, after 35 minutes of anodization, where the monitored potentials are above 4 V, the arc of the hemicircular shape decreases because of the decrease in the real part value ( $Z'$ ) parallel to the capacitive component. The deflection occurred at about 4 V of the measured potential, as shown in Figure 2b. Bardwell *et al.* also observed a break in the curve of the thickness of the anodic oxide formed potentiostatically as a function of anodic voltage at about 3.5 V, and suggested a possible second mechanism of film growth at potentials higher than 3.5 V.<sup>17</sup>

An appropriate description of the EOS structure in terms of an equivalent circuit is shown in Figure 5a.<sup>13,18</sup>  $C_{sc}$  is the space-charge capacitance,  $R_{sc}$  the space-charge resistance,  $C_{ss}$  the surface state capacitance, and  $R_{ss}$  the surface state resistance, assuming that the double layer capacitance ( $C_{dl}$ ) can be neglected ( $C_{dl} \gg C_{sc}$  and  $C_{ox}$ ). The equivalent circuit in Figure 5a can be greatly simplified if the surface-state contribution can also be neglected (Figure 5b). Space charge capacitance of the accumulation layer and its parallel resistance of the semiconductor Si electrode are included in the

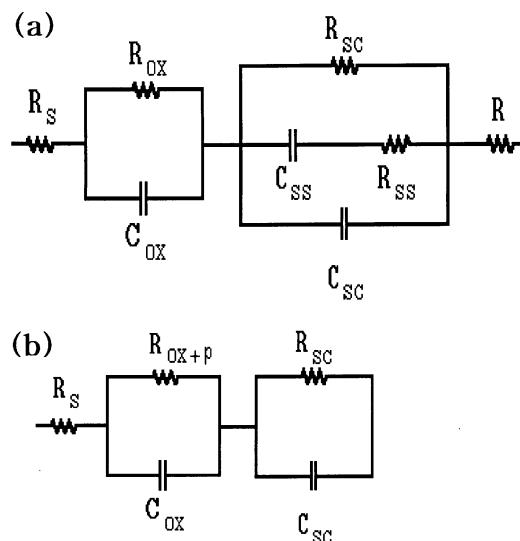


Figure 5. Equivalent circuits of the electrolyte/oxide/semiconductor (EOS) interfaces.

equivalent circuit in series with the thin  $\text{SiO}_2$  layer capacitance and its resistance to fit the measured impedance data. Anodic oxide films exhibit a nonideal capacitive behavior, and hence a constant phase element (CPE) has to be introduced for the evaluation of the experimental results in terms of an equivalent circuit.<sup>19</sup> The admittance ( $Y$ ) of a CPE is expressed in the form;  $Y_{\text{CPE}} = A(j\omega)^\alpha = A_0\omega^\alpha [\cos(\alpha\pi/2) + j\sin(\alpha\pi/2)]$ , where  $\omega = 2\pi f$  and  $-1 < \alpha < 1$ . A nonideal capacitive behavior, which is expressed by  $\alpha$  in the phase constants element correspondent to the  $\text{SiO}_2$ /electrolyte interface, decreases as the anodization time increases. For nonideal and/or leaky capacitors, the resistive component has to be introduced in parallel with the capacitor in the equivalent circuit, which is included in the  $R_{ox+p}$  resistance. The component values of the fitted equivalent circuits are listed in Table 1. When applying the anodic current of  $10 \mu\text{A}/\text{cm}^2$  in both aqueous and nonaqueous solutions, the capacitance values of the oxide layer increase slightly as the anodization time increases, even if the oxide layer does not seem to grow after 5 minutes anodization. This phenomenon would indicate that the surface becomes rough by dissolution and regrowth of the film as the anodization proceeds in solution, which results in the increase in the surface area. When applying an anodic current of  $30 \mu\text{A}/\text{cm}^2$ , the capacitance of the oxide ( $C_{ox}$ ) decreases somewhat (continuously) as the anodization proceeds in both aqueous and nonaqueous solutions. The thickness of the oxide layer has been estimated from the capacitance of the oxide by the equation,  $C_{ox} = f_R A \epsilon_0 \epsilon / d$ , where  $f_R$  represents the surface roughness factor,  $A$  the surface area,  $\epsilon_0$  the vacuum permittivity ( $8.85 \times 10^{-12}$ ), the dielectric constant of  $\text{SiO}_2$  (4.42),  $\epsilon$  and  $d$  the thickness of the oxide layer.<sup>13</sup> The surface roughness factor,  $f_R$ , is considered to be inversely proportional to the nonideality factor,  $\alpha$ , of the capacitor of the oxide layer. The thickness of the dielectric  $\text{SiO}_2$  layer calculated from the capacitance ( $C_{ox}$ ) is also listed in Table 1. The oxide grows

**Table 1.** Electrical component values of the equivalent circuit fitted to the measured impedance data

Electrolyte	Current density	Anodization time (min.)	Component values of the equivalent circuit								SiO <sub>2</sub> thickness (Å)	Ellipsometrically estimated values(Å)		
			R <sub>sc</sub> (KΩ)	C <sub>sc</sub>		R <sub>ox+p</sub> (M)	C <sub>ox</sub>		R <sub>s</sub> (Ω)					
				nF/cm <sup>2</sup>	α		nF/cm <sup>2</sup>	α						
H <sub>2</sub> O (1.35M NH <sub>3</sub> )	10 μA/cm <sup>2</sup>	5	21.1	59.1	0.94	2.2	1493	0.98	535	26.7	50.7			
		20	16.5	61.4	0.91	3.4	1558	0.98	539	25.6				
		40	14.6	64.6	0.88	3.1	1660	0.98	501	24.0				
		60	14.9	70.6	0.88	4.0	1564	0.97	477	25.7				
	30 μA/cm <sup>2</sup>	5	12.7	56.8	0.94	6.4	1612	0.98	510	24.8	103.0			
		20	13.0	62.2	0.91	18.5	1434	0.98	504	27.7				
		30	12.7	67.2	0.89	25.9	1242	0.98	503	32.2				
		40	11.9	70.8	0.89	20.4	982	0.96	484	41.5				
		50	11.5	74.9	0.89	13.5	778	0.94	446	53.5				
		60	10.7	81.2	0.88	8.6	542	0.90	427	79.9				
		C <sub>2</sub> H <sub>6</sub> O <sub>2</sub> (0.04M KNO <sub>3</sub> )	10 μA/cm <sup>2</sup>	5	13.8	60.9	0.92	6.43	1502	0.98		1.21k	26.4	53.3
				20	13.3	59.8	0.92	49.4	1518	0.98		1.85k	26.1	
40	13.8			59.1	0.92	49.4	1577	0.99	1.87k	25.0				
60	13.4		59.7	0.92		1586	0.99	1.89k	24.9					
30 μA/cm <sup>2</sup>	5		25.1	54.1	0.94	16.7	1322	0.99	2.00k	29.9				
	20		23.8	53.4	0.94	58.3	1311	0.99	2.11k	29.9				
	40	23.5	52.8	0.94	159.4	1250	0.99	2.09k	31.3					
	60	23.1	52.1	0.93	192.2	1111	0.99	2.31k	35.3	59.0				

better in aqueous solution than in ethylene glycol solution at the anodic current density of 30 μA/cm<sup>2</sup>. Especially, the oxides grow efficiently above the anodization potential of water. Current densities higher than 30 μA/cm<sup>2</sup> could cause an abrupt oxidation of the silicon surfaces, resulting in oxide layers having multiple defects from occlusion and mechanical entrapment. The thickness of the oxides was also measured after the anodic growth by ellipsometry and compared with those derived from the impedance measurements. In ellipsometric determination of the thickness for the ultrathin dielectric film, measurement error in thickness can be introduced by the uncertain in the refractive index of the film. The thicknesses estimated from the impedance data is generally lower than those determined from ellipsometry. The difference in the oxide thickness measured by ellipsometry and impedance may be in part due to surface roughness, which increases the effective area and thus may lead to an increase in the measured surface capacitance. Hence, without taking into account the exact surface roughness, the thickness calculated from the measured capacitance is too low. Also, the difference in the thicknesses is in part due to the difference between the two measurements. For impedance measurement the measured thickness would be the thinnest part of the film, on the other hand, for ellipsometry the average thickness is measured.

The sum of the oxide resistance and the anodic polarization resistance (R<sub>ox+p</sub>) increases continuously and infinitely with the anodization in ethylene glycol solution. As discussed earlier, the polarization resistance for the oxidation of silicon in nonaqueous solutions increases to an infinite value because of the anodic polarization of the oxygen supplier

(mostly H<sub>2</sub>O) in the electrolyte either to make Si-O bonds on the surfaces or to evolve oxygen molecules. At these low current densities and voltages, ethylene glycol cannot be decomposed to donate the oxygen atoms or ions to the silicon surfaces easily as mentioned earlier. However, R<sub>ox+p</sub> in aqueous solution increases up to about 4 V and then decreases. Since the oxide is continuously formed and the oxide resistance is expected to increase continuously, the anodic polarization resistance must increase up to about 4 V and decrease above that potential. Above 4 V for the anodic potential, the polarization resistance of oxygen evolution is expected to decrease, since oxygen molecules evolve abundantly at the electrode surfaces. In addition, the oxygen molecule is expected to dissolve interstitially into SiO<sub>2</sub> films. Oxygen transport is known to take place by interstitially dissolved oxygen molecules that exchange freely with network oxygen in thermal oxidation processes.<sup>20</sup> In anodic oxidation processes, the interstitially dissolved oxygen molecules in SiO<sub>2</sub> lattices can also facilitate the formation of the SiO<sub>2</sub> layer at the interfaces. Hence, the polarization resistance of the oxide formation decreases and the oxides grow efficiently above the anodization potential of water.

### Summary

Electrochemical oxidation of silicon (p-type(100)) at room temperature in ethylene glycol and in aqueous solution has been processed galvanostatically with low current densities for the preparation of SiO<sub>2</sub> layers. *In-situ* ac impedance methods have been employed for the characterization of the EOS interface and to investigate the growth of the anodic

oxides. The impedance for the lower frequency region changes characteristically depending on the applied current and on the electrolytes. Equivalent circuits corresponding to the EOS interfaces have been worked out to fit the measured impedance data, and the oxide layer thicknesses have been calculated from the oxide layer capacitances ( $C_{ox}$ ). The thickness of  $SiO_2$  layers calculated from the capacitance was in the range of 25-100 Å depending on the experimental condition. In aqueous ammonia solutions, when the monitored potential increases above ca. 4 V, the trend of component values for the simulated equivalent circuit changes. The anodic polarization resistance ( $R_p$ ) in the equivalent circuits decreases above this potential. Above this potential, oxygen molecules evolve by the oxidation of water at the electrode surfaces. In anodic oxidation processes, the interstitially dissolved oxygen molecules in  $SiO_2$  lattices are expected to facilitate the formation of  $SiO_2$  at the interfaces. Hence, the polarization resistance decreases and the oxide layers grow efficiently above the anodization potential of water. Thin  $SiO_2$  films grow efficiently at a controlled rate when low anodization currents in aqueous solutions are applied.

**Acknowledgment.** This work has been supported in part by a special fund for University Research Institute, Korea Research Foundation and in part by the Korea Science and Engineering Foundation (96-0501-05-01-3).

### References

1. Lewerenz, H. Z. *Electrochimica Acta* **1992**, 37, 847.
2. Cahill, D. G.; Avouris, Ph. *Appl. Phys. Lett.* **1992**, 60, 326.
3. Deal, B. E.; Grove, A. S. *J. Appl. Phys.* **1965**, 36, 3770.
4. Khemka, V.; Chow, T. P. *J. Electrochem. Soc.* **1997**, 144, 1137.
5. Fung, T. F.; Wong, H.; Cheng, Y. C.; Pun, C. K. *J. Electrochem. Soc.* **1991**, 138, 3747.
6. Revesz, A. G. *J. Electrochem. Soc.* **1967**, 114, 629.
7. Duffek, E. F.; Mylroie, C.; Benjamini, E. A. *J. Electrochem. Soc.* **1964**, 111, 1042.
8. Clark, K. B.; Bardwell, J. A.; Baribeau, J. M. *J. Appl. Phys.* **1994**, 76, 3114.
9. Mende, G.; Hensel, H.; Fenske, F.; Flietner, H. *Thin Solid Films* **1989**, 168, 51.
10. Mende, G. *J. Electrochem. Soc.* **1980**, 127, 2086.
11. Landheer, D.; Bardwell, J. A.; Clark, K. B. *J. Electrochem. Soc.* **1994**, 141, 1309.
12. Croset, M.; Petreanu, E.; Samuel, D.; Amsel, G.; Nadai, J. P. *J. Electrochem. Soc.* **1971**, 118, 717.
13. Schmuki, P.; Bohni, H.; Bardwell, J. A. *J. Electrochem. Soc.* **1995**, 142, 1705.
14. Glembocki, O. J. *SPIE Vol. 452 Spectroscopic Characterization Techniques for Semiconductor Technology*; 1983; p 130.
15. Hdiy, A. El.; Salace, G.; Petit, C.; Jourdain, M.; Meinerzhagen, A. *J. Appl. Phys.* **1993**, 73, 3569.
16. Chazalviel, J.-N. *Electrochimica Acta* **1992**, 37, 865.
17. Bardwell, J. A.; Clark, K. B.; Mitchell, D. F.; Bisaillon, D. A.; Sproule, G. I.; MacDougall, B.; Graham, M. J. *J. Electrochem. Soc.* **1993**, 140, 2135.
18. Sze, S. M. *Physics of Semiconductor Devices*, 2<sup>nd</sup> ed.; John Wiley & Sons, Inc.: New York, 1981.
19. Macdonald, J. R. *Impedance Spectroscopy*; John Wiley & Sons, Inc.: New York, 1987.
20. Atkinson, A. *Rev. Mod. Phys.* **1985**, 57, 437.